Monthly Notices
of the
ROYAL ASTRONOMICAL SOCIETY

MNRAS **471,** 532–540 (2017)
Advance Access publication 2017 June 30

doi:10.1093/mnras/stx1619

Lifetime measurements using two-step laser excitation for high-lying even-parity levels and improved theoretical oscillator strengths in Y II

P. Palmeri,[1⋆] P. Quinet,[1,2] H. Lundberg,[3] L. Engström,[3] H. Nilsson[4] and H. Hartman[4,5]

[1]*Physique Atomique et Astrophysique, Université de Mons - UMONS, 20 Place du Parc, B-7000 Mons, Belgium*
[2]*IPNAS, Université de Liège, Campus du Sart-Tilman, B-4000 Liège, Belgium*
[3]*Department of Physics, Lund University, Box 118, SE-221 00 Lund, Sweden*
[4]*Lund Observatory, Lund University, Box 43, SE-221 00 Lund, Sweden*
[5]*Material Sciences and Applied Mathematics, Malmö University, SE-205 06 Malmö, Sweden*

Accepted 2017 June 23. Received 2017 June 23; in original form 2017 March 16

ABSTRACT

We report new time-resolved laser-induced fluorescence lifetime measurements for 22 highly excited even-parity levels in singly ionized yttrium (Y II). To populate these levels belonging to the configurations 4d6s, 5s6s 4d5d, $5p^2$, 4d7s and 4d6d, a two-step laser excitation technique was used. Our previous pseudo-relativistic Hartree–Fock model (Biémont et al. 2011) was improved by extending the configuration interaction up to $n = 10$ to reproduce the new experimental lifetimes. A set of semi-empirical oscillator strengths extended to transitions falling in the spectral range λλ194–3995 nm, depopulating these 22 even-parity levels in Y II, is presented and compared to the values found in the Kurucz's data base (Kurucz 2011).

Key words: atomic data – atomic processes – methods: numerical.

1 INTRODUCTION

Accurate oscillator strengths for electric dipole transitions in Y II are needed for the determination of the yttrium abundance in stellar atmospheres. A recent example is the determination of the abundance ratio [Y/Mg] in solar twins that provides a sensitive chronometer for Galactic evolution (Nissen 2015; Tucci Maia et al. 2016). Yttrium ($Z = 39$) is a slow neutron-capture element primarily produced in low-to-medium mass AGB stars at solar metallicity, and its presence in stars of different ages and locations gives a good indication of the chemical history of the Milky Way (Mishenina et al. 2016).

High-excitation lines have additional diagnostic value because they can probe both non-local thermodynamical equilibrium and 3D effects in stellar atmospheres (Lind, Bergeman & Asplund 2012). It is worth noting that all previous experimental lifetimes and oscillator strengths available in the literature for Y II only involve low-excited odd-parity levels (Andersen, Ramanujan & Bahr 1978; Hannaford et al. 1982; Gorshklov & Komarovskii 1986; Pitts & Newson 1986; Wännström et al. 1988; Reshetnikova & Skorokhod 1999; Biémont et al. 2011). With the exception of the Kurucz's data base (Kurucz 2011), this is also the case for the theoretical data (Pirronello & Strazzulla 1980; Migdalek & Baylis 1987; Migdalek & Stanek 1993; Biémont et al. 2011). Hannaford et al. (1982) combine the experimental lifetimes with relative intensities of the lines depopulating these levels to derive oscillator strengths.

The aim of this study is to extend our knowledge of Y II to include highly excited even-parity levels. This was accomplished with a two-step laser excitation technique at the Lund High Power Laser Facility VUV laboratory using time-resolved laser-induced fluorescence (TR-LIF). Our previous HFR+CPOL calculations (Biémont et al. 2011) have been extended up to $n = 10$ to provide the radiative rates for the transitions depopulating the whole set of measured odd-parity and even-parity levels.

In Section 2, a description of the experimental method is given. Section 3 describes our new HFR+CPOL calculations. The results are presented and discussed in Section 4.

2 TR-LIF MEASUREMENTS

The ground state in Y II is $5s^2\ ^1S_0$ and the lowest excited term is $4d5s\ ^3D$, with levels below 1500 cm^{-1}. These even-parity levels are directly populated in the ablation plasma created by focusing a frequency doubled Nd:YAG laser on a rotating yttrium target inside a vacuum chamber with a pressure of about 10^{-4} mbar. To reach the highly excited even-parity levels, we applied a two-step procedure. A Nd:YAG pumped dye laser, with a pulse length of around 10 ns and operating on a Pyridin dye, excited the intermediate odd-parity levels in the 4d5p configuration around 29 000 cm^{-1}. A second Nd:YAG pumped dye laser, with a pulse length of 0.8 ns and operating on DCM dye, excited the final, even-parity levels, in the energy range 50 000–75 000 cm^{-1} studied in this investigation. An

⋆ E-mail: patrick.palmeri@umons.ac.be

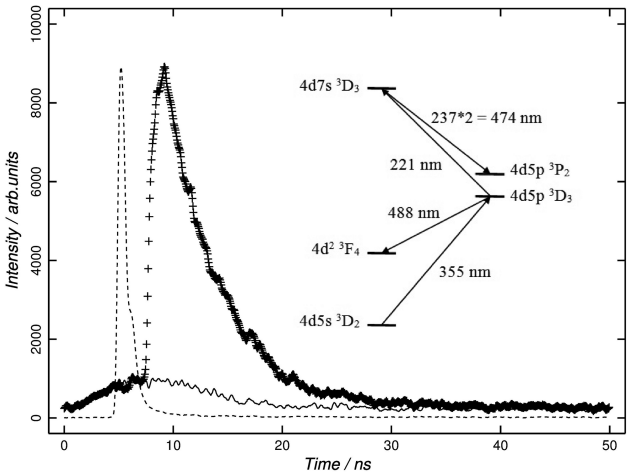

Figure 1. The + signs show the measured decay of the 4d7s $^3D_3$ level in Y II in the second spectral order at 474 nm, perturbed by the first-order decay from the intermediate 4d5p $^3D_3$ level at 488 nm. The insert illustrates schematically the excitation and decay channels involved. The lower curve (solid line) is a separate measurement at 474 nm with the second-step laser blocked, revealing the perturbation. This curve is then subtracted from the actual decay measurement. The dashed curve shows the second-step excitation laser, with a full width at half-maximum of 0.8 ns and displaced in time for clarity.

example of the two-step procedure is shown schematically in the insert in Fig. 1. Details of the set-up at the high-power laser facility in Lund are given by Lundberg et al. (2016), and an overview is presented in fig. 1 of that paper.

To reach the 4d5p levels, wavelengths around 350 nm were obtained by frequency doubling of the dye-laser output in a KDP crystal. For the final step, we utilized frequency doubling or tripling and, when necessary, added or subtracted one Stokes shift of 4153 cm^{-1} in a H_2 gas cell. The fluorescence from the excited levels was detected by a 1/8 m monochromator, with its 0.12 mm wide entrance slit oriented parallel to the excitation laser beams and perpendicular to the ablation laser, and registered by a fast micro-channel-plate PM-tube (Hamamatsu R 3809U) with a rise time of 200 ps. A Tektronix oscilloscope (DPO 7254) digitized both the fluorescence signal and the shape of the second-step excitation laser, recorded by a fast photodiode, in time steps of 50 ps. The different excitation and detection schemes used are presented in Table 1.

Each recorded decay curve was averaged over 1000 laser shots, and for each level we performed between 10 and 20 measurements over several days. All curves were analysed by fitting a single exponential decay convoluted by the recorded laser pulse and a constant background using the code DECFIT (Palmeri et al. 2008). The final lifetime is the average over all measurements, and is presented in Table 2. The quoted uncertainties include statistical uncertainties from the curve fitting and the variation between the repeated measurements, where the latter is the dominating source.

As discussed by Lundberg et al. (2016), there are two special experimental considerations in a two-step scheme. A problem may arise if there is a decay channel from the intermediate level close in wavelength to the channel used to measure the decay of the final level. Since the intermediate fluorescence is usually very intense and extends over more than 10 ns, this may cause problems even with a fairly large wavelength separation. One such case is illustrated in Fig. 1. Here, the transition at 488 nm from the intermediate

Table 1. Two-step excitation schemes in Y II.

Final level	First-step excitation[a] Start level[b] (cm^{-1})	Intermediate[b] (cm^{-1})	λ_{air} (nm)	Second-step excitation Final level[b] (cm^{-1})	λ_{air} (nm)	Scheme[c]	Detection λ^d_{air} (nm)
4d6s e^3D_1	1045	28 730	361.12	54 956.08	381.19	2ω+S	347
4d6s e^3D_2	1045	28 730	361.12	55 032.35	380.09	2ω+S	346[e], 461
4d6s e^3D_3	1045	28 730	361.12	55 645.64	371.43	2ω+S	428
4d6s e^1D_2	0	27 516	363.31	55 725.52	354.40	2ω+S	338[e], 446
5s6s e^3S_1	0	27 516	363.31	58 263.24	325.15	2ω	297, 384
4d5d e^1F_3	1449	28 394	371.02	58 533.30	331.70	2ω	309
4d5d f^3D_1	1045	28 595	362.87	58 720.38	331.85	2ω	307, 375[e]
5p^2 e^3P_0	1045	28 595	362.87	58 776.42	331.23	2ω	286
4d5d f^3D_2	1045	28 595	362.87	58 947.62	329.37	2ω	318, 373[e]
5p2 e^3P_1	1045	28 730	361.12	59 147.56	328.66	2ω	280, 283, 290
4d5d e^3G_3	1045	29 214	354.91	59 179.59	333.62	2ω	303, 313
4d5d f^3D_3	1045	29 214	354.91	59 327.89	331.98	2ω	311, 314
4d5d e^3G_4	1045	29 214	354.91	59 472.65	330.39	2ω	313
5p^2 e^3P_2	1045	29 214	354.91	59 670.26	328.24	2ω	278, 285
4d5d e^1P_1	1045	28 595	362.87	59 716.84	321.23	2ω	298, 308, 310
4d5d e^3G_5	1449	28 394	371.02	59 900.52	317.30	2ω	317
5p^2 f^1D_2	1045	28 730	361.12	60 535.92	314.32	2ω	278, 303
4d5d f^3P_1	1045	28 730	361.12	64 263.74	281.34	2ω+AS	281, 312
4d5d f^3P_2	1045	29 214	354.91	64 597.24	282.54	2ω+AS	282, 309
4d7s $^3D_3$	1045	29 214	354.91	74 374.91	221.36	3ω	237[e]
4d7s $^1D_2$	1045	29 214	354.91	74 582.56	220.35	3ω	242
	1045	28 730	361.12		218.02	3ω	242
4d6d $^3D_3$	1045	29 214	354.91	76 178.28	212.86	3ω	228

Notes. [a]For all measured levels, the first excitation step used the frequency doubled (2ω) output from the dye laser.
[b]Nilsson et al (1991).
[c]2ω/3ω means the frequency doubled/tripled output from the dye laser. S/AS is one added/subtracted Stokes shift of 4153 cm^{-1}.
[d]Fluorescence measurements below 400 nm were performed in the second spectral order.
[e]Corrected for fluorescence from the level excited by the first-step laser. See Fig. 1 and discussion in the text for further details.

Table 2. Comparison between experimental and theoretical lifetimes of selected levels in Y II.

Level[a]	Energy[a] (cm^{-1})	Experimental lifetime (ns) This work[b]	Experimental lifetime (ns) Others	Theoretical lifetime (ns) This work[c]	Theoretical lifetime (ns) Others
$5s5pz\,^3P^o_0$	23 445.063		54.7 ± 1.0[e]	64.48	31.88[h]
					38.31[i]
$5s5pz\,^3P^o_1$	23 776.245		51.5 ± 1.0[e]	57.52[j]	31.60[h]
					37.31[i]
$5s5pz\,^3P^o_2$	24 647.121		56.8 ± 1.0[e]	75.66[j]	33.41[h]
					42.74[i]
$4d5pz\,^1D^o_2$	26 147.252		5.9 ± 0.6[d]	5.94	5.67[h]
			6.3 ± 0.2[e]		5.32[i]
			6.82 ± 0.05[f]		
			6.7 ± 0.5[g]		
$4d5pz\,^3F^o_2$	27 227.027		6.8 ± 0.8[d]	5.67	5.46[h]
			6.3 ± 0.3[e]		5.08[i]
$4d5pz\,^1P^o_1$	27 516.699		5.6 ± 0.4[d]	6.32	5.58[h]
			5.0 ± 2.0[e]		4.93[i]
$4d5pz\,^3F^o_3$	27 532.321		5.9 ± 0.7[d]	5.83	5.42[h]
			6.3 ± 0.3[e]		5.21[i]
$4d5pz\,^3F^o_4$	28 394.177		6.0 ± 0.4[d]	5.51	5.17[h]
			5.7 ± 0.3[e]		4.91[i]
$4d5pz\,^3D^o_1$	28 595.285		4.5 ± 0.3[e]	4.08	3.98[h]
			4.58 ± 0.05[f]		3.65[i]
$4d5pz\,^3D^o_2$	28 730.010		5.8 ± 0.8[d]	4.01	3.80[h]
			4.3 ± 0.3[e]		3.52[i]
			4.53 ± 0.09[f]		
			6.4 ± 0.6[g]		
$4d5pz\,^3D^o_3$	29 213.958		5.2 ± 0.7[d]	3.93	3.75[h]
			4.4 ± 0.3[e]		3.46[i]
			4.43 ± 0.11[f]		
			5.7 ± 0.8[g]		
$4d5py\,^3P^o_0$	32 048.788		3.4 ± 0.2[e]	2.55	2.66[h]
			2.87 ± 0.04[f]		2.38[i]
			2.8 ± 0.2[h]		
$4d5py\,^3P^o_1$	32 124.054		4.2 ± 0.4[d]	2.55	2.67[h]
			3.3 ± 0.2[e]		2.38[i]
			2.87 ± 0.07[f]		
			2.8 ± 0.2[h]		
$4d5py\,^3P^o_2$	32 283.420		3.8 ± 0.2[d]	2.53	2.68[h]
			3.6 ± 0.2[e]		2.37[i]
			3.08 ± 0.10[f]		
			2.6 ± 0.2[h]		
$4d5pz\,^1F^o_3$	33 336.727		6.9 ± 0.7[d]	5.08	4.86[h]
			5.49 ± 0.09[f]		4.65[i]
			4.7 ± 0.3[h]		
$5s5py\,^1P^o_1$	44 568.540		1.2 ± 0.2[h]	1.05	0.99[h]
					0.89[i]
$4d6se\,^3D_1$	54 956.083	3.15 ± 0.15		3.46	3.16[i]
$4d6se\,^3D_2$	55 032.349	3.17 ± 0.15		3.61	3.28[i]
$4d6se\,^3D_3$	55 645.642	3.20 ± 0.15		3.52	3.14[i]
$4d6se\,^1D_2$	55 725.522	3.14 ± 0.15		4.38[j]	3.46[i]
$5s6se\,^3S_1$	58 263.238	2.61 ± 0.10		2.93	2.70[i]
$4d5de\,^1F_3$	58 533.296	2.43 ± 0.10		2.87	2.23[i]
$4d5df\,^3D_1$	58 720.382	2.60 ± 0.15		2.88	2.40[i]
$5p^2e\,^3P_0$	58 776.425	1.77 ± 0.09		1.96	2.20[i]
$4d5df\,^3D_2$	58 947.625	2.53 ± 0.10		2.95	2.56[i]
$5p^2e\,^3P_1$	59 147.559	1.92 ± 0.10		2.00	2.24[i]
$4d5de\,^3G_3$	59 179.589	2.53 ± 0.15		2.72	2.13[i]
$4d5df\,^3D_3$	59 327.880	2.64 ± 0.15		3.00	2.51[i]
$4d5de\,^3G_4$	59 472.643	2.45 ± 0.15		2.75	2.14[i]
$5p^2e\,^3P_2$	59 670.257	2.29 ± 0.10		2.10	2.39[i]
$4d5de\,^1P_1$	59 716.843	2.64 ± 0.10		3.03	2.40[i]
$4d5de\,^3G_5$	59 900.516	2.59 ± 0.10		2.81	2.19[i]
$5p^2f\,^1D_2$	60 535.922	4.36 ± 0.20		5.55[j]	5.00[i]
$4d5df\,^3P_1$	64 263.741	1.30 ± 0.07		1.60	0.94[i]
$4d5df\,^3P_2$	64 597.237	1.23 ± 0.05		1.55	0.93[i]

Table 2 – *continued*

Level[a]	Energy[a] (cm^{-1})	Experimental lifetime (ns) This work[b]	Other works	Theoretical lifetime (ns) This work[c]	Other works
$4d7s^3D_3$	74 374.907	4.11 ± 0.30		6.20[j]	5.99[j]
$4d7s^1D_2$	74 582.562	4.40 ± 0.30		6.32[j]	6.10[j]
$4d6d^3D_3$	76 178.282	3.76 ± 0.20		8.56[j]	7.25[j]

Notes. [a]Nilsson et al. (1991).
[b]TR-LIF measurements (see the text).
[c]HFR+CPOL calculations (see the text).
[d]Gorshklov & Komarovskii (1986), retarded coincidence in intersecting atomic and electron beams
[e]Hannaford et al. (1982), laser-induced fluorescence on sputtered metal vapour.
[f]Wännström et al. (1988), beam-laser technique.
[g]Andersen et al. (1978), beam-foil and sputtering excitation techniques.
[h]Biémont et al. (2011), laser-induced fluorescence on laser produced plasma.
[i]Kurucz (2011), semi-empirical calculations.
[j]Affected by strong cancellation effects, see discussion in text.

4d5p $^3D_3$ level is sufficiently close to the decay of the 4d7s $^3D_3$ level, which we measured in the second spectral order at 474 nm, to give a noticeable contribution to the decay curve, as seen in Fig. 1. However, this can be accurately corrected for by recording a separate decay curve with the second-step laser blocked, which is then subtracted from the first measurement before the lifetime analysis. All levels were checked for this effect. Several other cases were encountered and corrected for in a similar way, as noted in Table 1.

A more serious problem is caused by so-called cascades. One example encountered in this work is in the decay of the 4d5d $^3D_1$ level at 58 720 cm^{-1}. Here, we measured in two channels, 306.9 and 374.8 nm, but had to omit a third possibility at 320.4 nm since this line is blended by a cascade transition at 320.3 nm arising from 5d5p $^3P_0$ populated from the 4d5d $^3D_1$ level by the 374.8 nm transition. Since such problems cannot be corrected, spectroscopic investigations must be made to avoid using any perturbed channels. In this respect the availability of the comprehensive term analysis of Y II by Nilsson, Johansson & Kurucz (1991) is invaluable, since it allows us to identify which decay channels might be affected.

3 HFR+CPOL CALCULATIONS

As our previous calculations in Y II (Biémont et al. 2011) were restricted to correlation up to $n = 6$, the present HFR+CPOL calculations have been extended to $n = 10$ to model the highly excited energy levels up to $n = 7$ measured in this study.

The pseudo-relativistic Hartree–Fock (HFR) method (Cowan 1981) incorporating a core-polarization correction (CPOL) to the Hartree–Fock potential and to the dipole operator (Quinet et al. 1999, 2002) has been used. The configurations considered in the configuration interaction (CI) expansions were the following: $5s^2 + 5sns$ ($n = 6-10$) + 5snd ($n = 4-10$) + 5sng ($n = 5-10$) + $4d^2$ + 4dns ($n = 6-10$) + 4dnd ($n = 5-10$) + 4dng ($n = 5-10$) + $5d^2$ + 5d6s + 5d6d + $5p^2$ + 5png ($n = 4-6$) + $6s^2$ + $6p^2$ + 6pnf ($n = 4-6$) for the even parity; 5snp ($n = 5-10$) + 5snf ($n = 4-10$) + 5snh ($n = 6-10$) + 4dnp ($n = 5-10$) + 4dnf ($n = 4-10$) + 4dnh ($n = 6-10$) + 5pnd ($n = 5-6$) + 6pnd ($n = 5-6$) for the odd parity. The ionic core considered for the core-polarization effects was a krypton-like yttrium $[Ar]3d^{10}4s^24p^6$ core with a static dipole polarizability of $\alpha_c = 4.05a_0^3$ (Johnsson, Kolb & Huang 1983) and a cut-off radius taken as the HFR mean radius of the outermost core orbital, i.e. $r_c = \langle 4p|r|4p\rangle_{HFR} = 1.453a_0$.

In a least-squares fitting procedure, some radial parameters have been adjusted to minimize the differences between the Hamiltonian eigenvalues and the experimental energy levels of Nilsson et al. (1991). The levels belong to the configurations $5s^2$, 5sns $n = 6-8$, 5snp $n = 5-6$, 5snd $n = 4-6$, 5snf $n = 4-5$, $4d^2$, 5dns $n = 6-9$, 5dnp $n = 5-7$, 5dnd $n = 5-8$, 5dnf $n = 4-7$, 5d5g and $5p^2$. The configuration average energies, E_{av}, the direct and exchange Slater integrals F^k and G^k, the effective interaction parameters (α, β and T) and the spin-orbit integrals ζ of these configurations have been fitted. Their fitted and ab initio values are reported in Table 3. All the other Slater integrals have been scaled down by a factor of 0.85.

In total, 119 even-parity and 115 odd-parity experimental energy levels published in Nilsson et al. (1991) have been included in the fitting procedure and the average deviations have been minimized to 158 cm^{-1} for the even-parity levels and to 118 cm^{-1} for the odd-parity levels.

4 RESULTS AND DISCUSSION

Our lifetimes are given in Table 2 and compared to available experimental and theoretical values.

For the odd-parity levels, our theoretical values are, in most of the cases, slightly larger than our previous calculations (Biémont et al. 2011), i.e. they are ∼5 to ∼15 per cent larger with the exception of the triplets 5s5p z^3P^o and 4d5p y^3P^o, and generally in better agreement with measurements. Some of the theoretical lifetimes are affected by strong cancellation effects (with cancellation factors as defined by Cowan 1981 less than 0.1) on decay channels that contribute significantly (more than 10 per cent) to the radiative lifetime. They are marked with an asterisk in Table 2 and are model sensitive. For instance, the three theoretical values are noticeably different for the level 5s5p $z^3P^o_2$ and the cancellation effects tend to lengthen the calculated lifetimes.

For the even-parity levels, our calculated values are on average slightly longer than our experimental ones by about 10 per cent. This means that the core-polarization effects are overestimated for the even-parity levels in our model. On the other hand, the lifetimes calculated by Kurucz (2011), who used Cowan's codes (Cowan 1981), are on average 5 per cent shorter than our measurements.

As for the odd levels, some lifetimes are significantly longer than our measurements by up to a factor two, notably for the level $4d6d^3D_3$. In our calculations, this is due to strong cancellation effects. Most likely this is also the case for the Kurucz data, although

Table 3. Radial parameters adopted in our HFR+CPOL model of the Y II atomic structure. All Slater and spin–orbit parameters not listed here have been respectively scaled down by 0.85 and fixed to their ab initio values.

Configuration	Parameter	Ab initio (cm^{-1})	Fitted (cm^{-1})	Ratio	Note[a]
		Even parity			
$5s^2$	E_{av}	4830	4944		
5s6s	E_{av}	59 972	60 082		
	G^0(5s6s)	2059	1740	0.845	
5s7s	E_{av}	80 350	80 089		
	G^0(5s7s)	666	579	0.850	F
5s8s	E_{av}	89 519	89 339		
	G^0(5s8s)	312	271	0.850	F
5s4d	E_{av}	2620	2905		
	ζ_{4d}	287	229	0.798	
	G^2(5s4d)	16 294	15 118	0.928	R1
5s5d	E_{av}	65 311	65 942		
	ζ_{5d}	42	42	1.000	F
	G^2(5s5d)	3580	3321	0.928	R1
5s6d	E_{av}	82 850	82 936		
	ζ_{6d}	17	17	1.000	F
	G^2(5s6d)	1298	1204	0.928	R1
$4d^2$	E_{av}	12 456	12 295		
	F^2(4d4d)	38 633	31 330	0.811	
	F^4(4d4d)	24 710	20 257	0.820	
	α	0	43		
	β	0	−879		
	T	0	3		
	ζ_{4d}	244	154	0.631	
4d6s	E_{av}	55 205	56 380		
	ζ_{4d}	313	215	0.687	R2
	G^2(4d6s)	2527	2344	0.928	R1
4d7s	E_{av}	73 557	74 073		
	ζ_{4d}	317	218	0.687	R2
	G^2(4d7s)	933	865	0.928	R1
4d8s	E_{av}	82 166	82 674		
	ζ_{4d}	318	218	0.687	R2
	G^2(4d8s)	460	426	0.928	R1
4d9s	E_{av}	86 934	87 585		
	ζ_{4d}	319	219	0.687	R2
	G^2(4d9s)	262	244	0.928	R1
4d5d	E_{av}	59 997	61 257		
	ζ_{4d}	313	302	0.965	R3
	ζ_{5d}	37	37	1.000	F
	F^2(4d5d)	7388	4988	0.675	R4
	F^4(4d5d)	3452	2331	0.675	R4
	G^0(4d5d)	4181	1958	0.468	R5
	G^2(4d5d)	3330	1559	0.468	R5
	G^4(4d5d)	2451	1148	0.468	R5
4d6d	E_{av}	75 859	76 512		
	ζ_{4d}	317	305	0.965	R3
	ζ_{6d}	15	15	1.000	F
	F^2(4d6d)	2847	1923	0.675	R4
	F^4(4d6d)	1323	892	0.675	R4
	G^0(4d6d)	1434	672	0.468	R5
	G^2(4d6d)	1241	581	0.468	R5
	G^4(4d6d)	938	439	0.468	R5
4d7d	E_{av}	83 423	84 070		
	ζ_{4d}	318	306	0.965	R3
	ζ_{7d}	8	8	1.000	F

Table 3 – *continued*

Configuration	Parameter	Ab initio (cm^{-1})	Fitted (cm^{-1})	Ratio	Note[a]
	F^2(4d7d)	1440	972	0.675	R4
	F^4(4d7d)	676	456	0.675	R4
	G^0(4d7d)	696	325	0.468	R5
	G^2(4d7d)	624	292	0.468	R5
	G^4(4d7d)	477	224	0.468	R5
4d8d	E_{av}	87 692	88 413		
	ζ_{4d}	319	307	0.965	R3
	ζ_{8d}	5	5	1.000	F
	F^2(4d8d)	836	565	0.675	R4
	F^4(4d8d)	396	268	0.675	R4
	G^0(4d8d)	396	185	0.468	R5
	G^2(4d8d)	362	170	0.468	R5
	G^4(4d8d)	278	130	0.468	R5
4d5g	E_{av}	80 522	81 390		
	ζ_{4d}	319	319	1.000	F
	ζ_{5g}	0	0	1.000	F
	F^2(4d5g)	906	788	0.850	F
	F^4(4d5g)	133	116	0.850	F
	G^2(4d5g)	32	28	0.850	F
	G^4(4d5g)	22	19	0.850	F
	G^6(4d5g)	16	14	0.850	F
$5p^2$	E_{av}	61 417	62 631		
	F^2(5p5p)	25 147	16 038	0.638	
	α	0	0		F
	ζ_{5p}	658	634	0.964	
		Odd parity			
5s5p	E_{av}	27 694	29 865		
	ζ_{5p}	654	960	1.468	R6
	G^1(5s5p)	31 781	23 177	0.729	R7
5s6p	E_{av}	69 782	69 960		
	ζ_{6p}	198	291	1.468	R6
	G^1(5s6p)	3948	2879	0.729	R7
5s4f	E_{av}	76 144	77 227		
	ζ_{4f}	0	0	1.000	F
	G^3(5s4f)	4283	3222	0.752	R8
5s5f	E_{av}	87 425	87 617		
	ζ_{5f}	0	0	1.000	F
	G^3(5s5f)	2138	1609	0.752	R8
4d5p	E_{av}	28 527	29 831		
	ζ_{4d}	299	259	0.866	R9
	ζ_{5p}	523	637	1.218	R10
	F^2(4d5p)	16 960	13 743	0.810	R11
	G^1(4d5p)	9651	8517	0.883	R12
	G^3(4d5p)	7271	6418	0.883	R12
4d6p	E_{av}	63 890	64 656		
	ζ_{4d}	314	273	0.866	R9
	ζ_{6p}	180	219	1.218	R10
	F^2(4d6p)	4914	3982	0.810	R11
	G^1(4d6p)	1939	1711	0.883	R12
	G^3(4d6p)	1674	1478	0.883	R12
4d7p	E_{av}	77 473	78 090		
	ζ_{4d}	317	275	0.866	R9
	ζ_{7p}	84	102	1.218	R10
	F^2(4d7p)	2101	1702	0.810	R11
	G^1(4d7p)	784	692	0.883	R12
	G^3(4d7p)	702	619	0.883	R12

Table 3 – *continued*

Configuration	Parameter	Ab initio (cm^{-1})	Fitted (cm^{-1})	Ratio	Note[a]
4d4f	E_{av}	69 478	70 790		
	ζ_{4d}	317	292	0.921	R13
	ζ_{4f}	0	0	1.000	F
	F^2(4d4f)	4349	3265	0.751	R14
	F^4(4d4f)	1534	1151	0.751	R14
	G^1(4d4f)	1743	1253	0.719	R15
	G^3(4*d*4*f*)	1014	729	0.719	R15
	G^5(4*d*4*f*)	699	502	0.719	R15
4d5f	E_{av}	80 041	80 958		
	ζ_{4d}	318	293	0.921	R13
	ζ_{5f}	0	0	1.000	F
	F^2(4d5f)	2069	1553	0.751	R14
	F^4(4d5f)	820	615	0.751	R14
	G^1(4d5f)	1087	781	0.719	R15
	G^3(4d5f)	639	459	0.719	R15
	G^5(4d5f)	443	318	0.719	R15
4d6f	E_{av}	85 675	86 502		
	ζ_{4d}	318	294	0.921	R13
	ζ_{6f}	0	0	1.000	F
	F^2(4d6f)	1165	875	0.751	R14
	F^4(4d6f)	488	366	0.751	R14
	G^1(4d6f)	680	488	0.719	R15
	G^3(4d6f)	403	289	0.719	R15
	G^5(4d6f)	278	200	0.719	R15
4d7f	E_{av}	89 048	89 844		
	ζ_{4d}	319	294	0.921	R13
	ζ_{7f}	0	0	1.000	F
	F^2(4d7f)	722	542	0.751	R14
	F^4(4d7f)	311	233	0.751	R14
	G^1(4d7f)	445	320	0.719	R15
	G^3(4d7f)	265	190	0.719	R15
	G^5(4d7f)	183	132	0.719	R15

[a]F: fixed parameter value; R*n*: fixed ratio between these parameters.

the cancellation factors are not available in Kurucz's data base (Kurucz 2011).

Table 4 is a sample of a bigger table listing the strongest 357 E1 decay channels (having an *A*-value greater than 10^4 s^{-1}) depopulating the levels for which the lifetime has ever been measured in Y II. Here, the transitions with $\lambda < 230$ nm are shown. The whole table is available in electronic format at the Centre de Données astronomiques de Strasbourg (CDS 2017) and in the online version of the paper as supplementary material. Along with the HFR+CPOL oscillator strengths ($\log gf$) and transition probabilities (gA), the corresponding corrected radiative parameters ($\log gf_c$ and gA_c) are given for each transition with the experimental lifetime of the upper level (τ_c) used to rescale these parameters. We recommend the astronomical community to use these rescaled values as they should correct the overestimation of the core-polarization effects by our model for the highly-excited even-parity levels involved in the transition outlined in the previous paragraph.

In Figs 2–4, the present HFR+CPOL oscillator strengths are compared with our previous values (Biémont et al. 2011), those of Kurucz (Kurucz 2011) and the experimental values of Hannaford et al. (1982), respectively. Although the latter concerns exclusively the decay transitions of low-lying odd-parity levels (Hannaford et al. 1982), they nonetheless provide a good test of the present HFR+CPOL model.

Fig. 2 shows a good agreement between our two calculations with no systematic effects, as the core-polarization has been taken into account in both models. However, some discrepancies are seen for the weak transitions due to cancellations such as the transition $4d^2a^2P_0-4d5pz^1P^o_1$ at 733.295 nm with $\log gf = -3.08$ and a cancellation factor of CF = 0.07 in this work, compared to $\log gf = -1.98$ obtained with our previous model. In this particular case, it is advisable to use our older published value (Biémont et al. 2011), i.e. −1.98, that belongs to a smaller set of calculated strong ($\log gf > -2$) decay transitions being not affected by cancellation. Besides, Kurucz (2011) gives a value of −2.87 for that line. We suspect that this oscillator strength is also affected by cancellation as it is calculated ∼1 dex weaker than the value of Biémont et al. (2011), similarly to the present calculation. Unfortunately, CF values are not reported in Kurucz (2011).

Fig. 3 shows that the oscillator strengths computed by Kurucz (2011) are systematically larger than ours by, on average, 0.07 dex for lines with $\log gf > 0$. Furthermore, a significant number (92 transitions out of 357) of the lines with $\log gf < 0$ are affected by strong cancellation effects (CF < 0.1) showing discrepancies of one dex or more. Using our $\log gf$-values with CF < 0.1 is not

Table 4. Transition probabilities (gA) and oscillator strengths (log gf) for the strongest (with an A-value greater than $10^4 s^{-1}$) decay channels depopulating the levels for which the lifetime has been measured in Y II. This is a sample for the transitions with $\lambda < 230$ nm. The complete table is available in electronic format at the CDS (2017) and in the online version of the paper as supplementary material.

λ^a (nm)	E^b_{low} (cm^{-1})	P^c_{low}	J_{low}	E^b_{up} (cm^{-1})	P^c_{up}	J_{up}	log gf	gA (s^{-1})	CF^d	log gf^e_c	gA^e_c (s^{-1})	τ^f_c (s)	Ref.^{g}
194.0573	24 647	(o)	2	76 178	(e)	3	−2.03	1.66E+07	0.030	−1.67	3.78E+07	3.76E − 09	T
199.8760	26 147	(o)	2	76 178	(e)	3	−2.00	1.68E+07	0.021	−1.64	3.82E+07	3.76E − 09	T
200.1937	24 647	(o)	2	74 583	(e)	2	−2.70	3.34E+06	0.056	−2.53	4.91E+06	4.30E − 09	T
201.0298	24 647	(o)	2	74 375	(e)	3	−2.84	2.35E+06	0.003	−2.66	3.55E+06	4.11E − 09	T
204.2193	27 227	(o)	2	76 178	(e)	3	−1.54	4.63E+07	0.077	−1.18	1.05E+08	3.76E − 09	T
205.5011	27 532	(o)	3	76 178	(e)	3	−2.29	8.08E+06	0.043	−1.93	1.84E+07	3.76E − 09	T
206.3950	26 147	(o)	2	74 583	(e)	2	−1.09	1.28E+08	0.159	−0.92	1.88E+08	4 .30E − 09	T
207.2838	26 147	(o)	2	74 375	(e)	3	−4.21	9.53E+04	0.005	−4.03	1.44E+05	4.11E − 9	T
209.2081	28 394	(o)	4	76 178	(e)	3	−1.84	2.24E+07	0.075	−1.48	5.09E+07	3.76E − 09	T
210.6890	28 730	(o)	2	76 178	(e)	3	−1.78	2.50E+07	0.076	−1.42	5.69E+07	3.76E − 09	T
211.1017	27 227	(o)	2	74 583	(e)	2	−1.13	1.11E+08	0.229	−0.96	1.63E+08	4.30E − 09	T
212.0315	27 227	(o)	2	74 375	(e)	3	−2.82	2.25E+06	0.187	−2.64	3.40E+06	4.11E − 09	T
212.4011	27 517	(o)	1	74 583	(e)	2	−3.50	4.76E+05	0.001	−3.33	6.99E+05	4.30E − 09	T
212.4716	27 532	(o)	3	74 583	(e)	2	−1.66	3.25E+07	0.304	−1.49	4.77E+07	4.30E − 09	T
212.8604	29 214	(o)	3	76 178	(e)	3	−1.19	9.60E+07	0.063	−0.83	2.18E+08	3.76E − 09	T
213.4136	27 532	(o)	3	74 375	(e)	3	−1.50	4.58E+07	0.350	−1.32	6.92E+07	4.11E − 09	T
217.3833	28 595	(o)	1	74 583	(e)	2	−2.51	4.42E+06	0.036	−2.34	6.49E+06	4.30E − 09	T
217.4143	28 394	(o)	4	74 375	(e)	3	−0.65	3.15E+08	0.355	−0.47	4.76E+08	4.11E − 09	T
218.0221	28 730	(o)	2	74 583	(e)	2	−1.93	1.65E+07	0.282	−1.76	2.42E+07	4.30E − 09	T
219.0141	28 730	(o)	2	74 375	(e)	3	−1.54	4.04E+07	0.442	−1.36	6.10E+07	4.11E − 09	T
220.3480	29 214	(o)	3	74 583	(e)	2	−2.81	2.13E+06	0.037	−2.64	3.13E+06	4.30E − 09	T
221.3613	29 214	(o)	3	74 375	(e)	3	−0.83	2.01E+08	0.426	−0.65	3.04E+08	4.11E − 09	T
224.3034	0	(e)	0	44 569	(o)	1	0.05	1.52E+09	0.359	0.08	1.32E+09	1.20E − 09	B
227.7468	32 283	(o)	2	76 178	(e)	3	−1.31	6.36E+07	0.084	−0.95	1.45E+08	3.76E − 09	T
228.6136	840	(e)	1	44 569	(o)	1	−4.03	1.22E+05	0.028	−4.00	1.06E+05	1.20E − 09	B
229.6898	1045	(e)	2	44 569	(o)	1	−2.70	2.58E+06	0.024	−2.67	2.25E+06	1.20E − 09	B

Notes. [a]Derived from the experimental energy levels in Nilsson et al. (1991). Wavelengths longer than 200 nm are given in air.
[b]Nilsson et al. (1991). Rounded to the last digit.
[c](e) and (o) stand for even and odd respectively.
[d]Cancellation factor (CF) as defined in Cowan (1981). The transition probability for which the CF is less than 0.1 is affected by a strong cancellation effect and should be taken with caution.
[e]Normalized using the experimental lifetime reported in the 13th column from the reference reported in the 14th column.
[f]Experimental lifetime of the upper level used to normalize the oscillator strength and the transition probability given respectively in columns 11 and 12.
[g]Reference of the experimental lifetime used to normalize the oscillator strength and the transition probability given respectively in columns 11 and 12. T = this work; B = Biémont et al. (2011); W = Wännström et al. (1988); H = Hannaford et al. (1982).

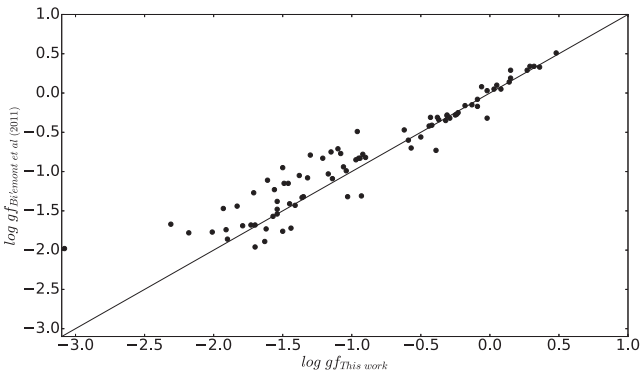

Figure 2. Comparison between the present HFR+CPOL log gf values and those of our previous study (Biémont et al. 2011). A straight line of equality has been drawn.

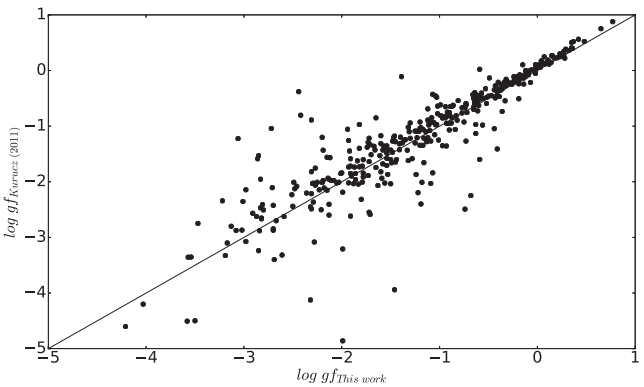

Figure 3. Comparison between the present HFR+CPOL log gf values and those of the Kurucz's data base (Kurucz 2011). A straight line of equality has been drawn.

recommended as these values could be off by a few dex. Moreover, values of Kurucz (2011) that are weaker than ours by a few dex should be taken with care as we suspect that they are affected by strong cancellation effects similarly to the case of the line at 733.295 nm discussed previously.

In Fig. 4, it is seen that our HFR+CPOL log gf-values agree well with the experimental determinations of Hannaford et al. (1982), the standard deviation of the differences between the two sets being 0.11 dex. From this comparison, one could estimate that the present

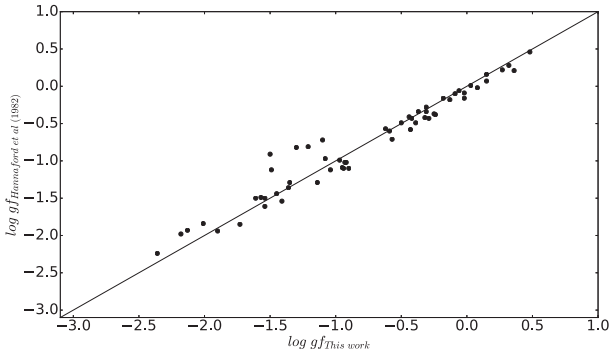

Figure 4. Comparison between the present HFR+CPOL log *gf* values and the experimental values of Hannaford et al. (1982). A straight line of equality has been drawn.

log *gf* values have an accuracy of the order of ∼0.1 dex with the exception of the HFR+CPOL values affected by cancellation, i.e. with CF < 0.1.

5 CONCLUSIONS

New lifetimes have been measured for 22 highly excited even-parity levels in Y II using TR-LIF spectroscopy. A two-step laser excitation method has been used to reach these levels that belong to the configurations 4d6s, 5s6s 4d5d, $5p^2$, 4d7s and 4d6d. To reproduce our measurements, particularly for the levels belonging to the 4d7s configuration, it was necessary to extend our previous HFR+CPOL model (Biémont et al. 2011) up to $n = 10$. Comparisons of the present HFR+CPOL calculations with previous and new measurements and theoretical data show a good agreement except for transitions affected by strong cancellations. In addition, it was found that the core-polarization effects in our model are slightly overestimated for the highly excited even-parity levels and consequently we choose to rescale our HFR+CPOL radiative rates using the experimental lifetimes for 357 E1 transitions in Y II.

ACKNOWLEDGEMENTS

This work was financially supported by the Integrated Initiative of Infrastructure Project LASERLAB-EUROPE, contract LLC002268, by the Belgian F.R.S.-FNRS, and by the Swedish Research Council through the Linnaeus grant to the Lund Laser Centre, project grant 2011-4206 and the Knut and Alice Wallenberg Foundation. PQ and PP are, respectively, Research Director and Research Associate of the F.R.S.-FNRS. The Belgian team is grateful to the Swedish colleagues for the warm hospitality enjoyed at the Lund Laser Centre during the two campaigns in 2016 June and August.

REFERENCES

Andersen T., Ramanujan P. S., Bahr K., 1978, ApJ, 223, 344
Biémont É. et al., 2011, MNRAS, 414, 3350
Centre de Données astronomiques de Strasbourg (CDS), 2017, available at: http://cds.u-strasbg.fr
Cowan R. D., 1981, The Theory of Atomic Structure and Spectra. Univ. California Press, Berkeley
Gorshklov V. N., Komarovskii V. A., 1986, Opt. Spectrosc., 60, 541
Hannaford P., Lowe R. M., Grevesse N., Biémont É., Whaling W., 1982, ApJ, 261, 736
Johnsson W. R., Kolb D., Huang K.-N., 1983, At. Data Nucl. Data Tables, 28, 333
Kurucz R. L., 2011, available at: http://kurucz.harvard.edu/atoms/3901
Lind K., Bergeman M., Asplund M., 2012, MNRAS, 427, 50
Lundberg H. et al., 2016, MNRAS, 460, 356
Migdalek J., Baylis W. E., 1987, Can. J. Phys., 65, 1612
Migdalek J., Stanek M., 1993, Z. Phys. D, 27, 9
Mishenina T. V., Korotin S. A., Carraro G., Kovtyukh V. V., Yegorova I. A., 2016, J. Phys. Conf. Ser., 665, 012025
Nilsson A. E., Johansson S., Kurucz R. L., 1991, Phys. Scr., 44, 226
Nissen P. E., 2015, A&A, 579, A52
Palmeri P., Quinet P., Fivet V., Biémont É., Nilsson H., Engström L., Lundberg H., 2008, Physica Scripta, 78, 015304
Pirronello V., Strazzulla G., 1980, Ap&SS, 72, 55
Pitts R. E., Newson G. H., 1986, J. Quant. Spectrosc. Radiat. Transfer, 35, 383
Quinet P., Palmeri P., Biémont É., McCurdy M. M., Rieger G., Pinnington E. H., Wickliffe M. E., Lawler J. E., 1999, MNRAS, 307, 934
Quinet P., Palmeri P., Biémont É., Li Z. S., Zhang Z. G., Svanberg S., 2002, J. Alloys Compd., 344, 255
Reshetnikova O. F., Skorokhod E. P., 1999, Opt. Spectrosc., 87, 829
Tucci Maia M., Ramírez I., Meléndez J., Bedell M., Bean J. L., Asplund M., 2016, A&A, 590, A32
Wännström A., Vogel O., Arnesen A., Hallin R., 1988, Phys. Scr., 38, 564

SUPPORTING INFORMATION

Supplementary data are available at *MNRAS* online.

etable4.txt

Please note: Oxford University Press is not responsible for the content or functionality of any supporting materials supplied by the authors. Any queries (other than missing material) should be directed to the corresponding author for the article.

This paper has been typeset from a TEX/LATEX file prepared by the author.